

Numerical Solutions of Fractional Covid-19 Model Using Spectral Collocation Method

Surath Ghosh^{*}, Sunil Kumar

*Department of Mathematics, National Institute of Technology,
Jamshedpur, 831014, Jharkhand, India*

Received 14 August 2021; Received in revised form 23 November 2021

Accepted 28 November 2021; Available online 30 December 2021

ABSTRACT

In this work, the mathematical model is considered on COVID-19 which makes the lives of people in the world into a hell. This present model has four components that are expressed as susceptible, exposed, infected and recovered (SEIR). Spectral collocation method (SCM) is presented here for numerical simulations because it is one of the important numerical technique having high rate convergence. Also, convergence analysis of the above method is presented here briefly. There is detailed description about the comparison of the rate of increasing of COVID-19 of India, Srilanka, Pakistan, Bangladesh respectively. If the four components are considered as zero initially, the effect of population to increase the disease is presented here.

Keywords: Convergence analysis; COVID-19; Mathematical modeling; Spectral collocation method

1. Introduction

The fractional calculus (FC) is an important part of calculus with the applications of fractional order integration and differentiation. The use of classical calculus and fractional calculus was initiated almost simultaneously. The idea of FC was first introduced by Leibniz and L'Hospital in 1695 as a semi derivative. Then FC was developed by many famous mathematicians like Euler, Laplace, Riemann, Letnikov and

many others. Now a days, we can say that there is no such disciplines in science, engineering, finance without the concept of FC. There are so many efficient methods in FC to express non-linear phenomena in the fields of physics and engineering [1]. Also, FC is used to express real life problems which have huge applications in so many field like economics [2], biology [3], digital circuits [4], cryptography [5] etc. Some recent applications of FC are described in

[6, 7].

The disease caused by Coronavirus is called COVID-19. Now, CO stands for the first two letters of Corona, VI is for first two letters of Virus and D comes for disease. Here, 19 means 2019, as this disease was first seen in Wuhan in December 2019. It is pandemic disease which is announced by WHO [8]. Now, it has spread quickly across the world. As there is still now no vaccine for it, social distancing is the most important way for controlling this disease [9]. There are so many countries those are badly affected by Coronavirus around the world [10, 11]. Some literatures are published on the epidemic characteristics of COVID-19 based on Wuhan, China [12, 13]. Special attention and care should be taken for the patients who has diabetes and COVID-19 [14].

Respiratory illness is caused by this disease with fever and cough. Difficulty in breathing is another most important symptoms in severe cases. We can keep safe ourself by washing our hands, not to touch our face, and keeping away from people who are already effected. Older people having high blood pressure, heart problems or diabetes are more likely to suffer serious illness.

This disease spreads basically through contact with an infected person when they sneeze or cough. The spreading rate is also increases due to touch a surface or object where this virus is already exist. Then if any people touches their eyes, nose, or mouth, got infected.

Still now there is some research articles to find the characteristics of infected patients with COVID-19. Around 41 cases were announced by Huang C in Wuhan in the Lancet on Jan 24, 2020. Yueling Ma et al. described the effects of humidity and temperature on the death of COVID-19 col-

lecting the data from 20 January, 2020 to 29 February, 2020 in Wuhan, China. In that work, author has applied Generalized additive model to get the results in [15]. Li Q has also reported 425 cases in Wuhan on Jan 29, 2020. The clinical characteristics of death cases with COVID-19 was presented by Xun Li et al. which helps to find critically ill patients early in [16]. Chen N presented characteristics of around 99 cases in Wuhan on Jan 30, 2020. There are some reserachers who has implemented a conceptual model for the coronavirus disease 2019 (COVID-19) in Wuhan, China [17]. Also Transmission network model is developed by TianMu Chen et al. in [18]. The details about COVID - 19 is described in [19–25]. There is a brief description about the effects of this disease in [26–33]. Some important results about this model are presented in [34–36]. This model simulate transmission from the bats infection to the human infection. In this work, we have considered COVID-19 model [37] as Caputo sense like

$$D_t^\alpha S(t) = a_1 - k_1 I(t)S(t)(1 + \alpha I(t)) - d_1 S(t). \tag{1.1}$$

$$D_t^\alpha E(t) = k_1 I(t)S(t)(1 + \alpha I(t)) - (d_1 + \gamma_1)E(t). \tag{1.2}$$

$$D_t^\alpha I(t) = b_1 + \gamma_1 E(t) - (d_1 + \beta_1 + \mu_1)I(t). \tag{1.3}$$

$$D_t^\alpha R(t) = \beta_1 I(t) - d_1 R(t). \tag{1.4}$$

The parameters which are used in the above COVID-19 model are described in Table1 in detail. In this case, the Caputo fractional operator is used due to it's good data fitting properties. Also, It is easy to use.

Spectral method is one of the high convergent numerical method which is applied mainly in applied mathematics. The basis function is applied due to it's orthogonality properties for approximating the

equations to get the solutions of the differential equations. The spectral-collocation method using Jacobi polynomial is presented by Yanping Chen et al. [38] with its convergence analysis. Also, solution of stochastic delay differential equations using spectral collocation method is described in [39] with the interpolation of Chebyshev polynomials. This method is presented to find the solutions of linear and non-linear fractional-order differential equations in [40]. In the present study, for approximating variable order fractional partial differential operator, authors has utilized Lagrange interpolation. Also a spectral pelanty method is implemented to explain the convergency of this method. Spectral method is developed to get solution of convection-reaction-diffusion equations having time fractional with the help of finite difference method [41]. Also, in this work stability and convergence analysis of the method are described briefly to get accurate and efficient results. The solution of nonlinear fractional differential equations is reported in [42] using spectral method.

The present work is sorted out as: In Section 2, the defination of fractional operator in Caputo sense is described. Then we have discussed about Chebyshev polynomial of 1st kind with its shifted forms in Section 3. There are some statements on convergence analysis of the described method in Section 4. In Section 5, detail about procedure of the method is presented. Also numerical simulations are illustrated briefly in Section 6. The conclusion statements are in Section 7.

2. Definitions and Preliminaries

Definition 2.1 ([43]). The fractional differential operator D^α of order α in Caputo

sense is expressed by

$$D^\alpha f(\eta) = \frac{1}{\Gamma(m-\alpha)} \int_0^\eta \frac{f^{(m)}(t)}{(\eta-t)^{\alpha-m+1}} dt, \tag{2.1}$$

where $m-1 < \alpha < m$, $m \in \mathbb{N}$, $\alpha > 0$, $\eta > 0$.

Caputo fractional derivative operator satisfies the linearity property like:

$$D^\alpha(\lambda f(\eta) + \mu g(\eta)) = \lambda D^\alpha f(\eta) + \mu D^\alpha g(\eta).$$

and it confirms the following property [44]

$$D^\alpha C = 0, \text{ where } C \text{ is a constant,}$$

$$D^\alpha \eta^n = \begin{cases} 0, & n < [\alpha]; \\ \frac{\Gamma(n+1)}{\Gamma(n+1-\alpha)} \eta^{n-\alpha}, & n \geq [\alpha]. \end{cases}$$

Where the smallest integer greater than or equal to α is denoted by $[\alpha]$ and $n \in \mathbb{N}_0$, with $\mathbb{N}_0 = 0, 1, 2, \dots$.

3. Chebyshev Spectral Method

The Chebyshev polynomials (CP) of first kind are explained on the interval $[-1, 1]$. This kind of CPs are expressed using the below recurrence relation [45] as

$$\zeta_{k+1}(\eta) = 2\eta\zeta_k(\eta) - \zeta_{k-1}(\eta),$$

$$k = 1, 2, 3, \dots,$$

where $\zeta_0(\eta) = 1$ and $\zeta_1(\eta) = \eta$. Now, we want to use these polynomials on the interval $[0, L]$ as shifted CPs. The transformation $\eta = \frac{2t}{L} - 1$ is taken for defining those kind of polynomial in the interval $[0, L]$. These kind of polynomials are denoted by $\zeta_k(\frac{2t}{L} - 1)$ with the recurrence relation as

$$\zeta_{k+1}^*(\eta) = 2\left(\frac{2t}{L} - 1\right)\zeta_k^*(\eta) - \zeta_{k-1}^*(\eta),$$

$$k = 1, 2, 3, \dots, \tag{3.1}$$

where $\zeta_0^*(\eta) = 1$, $\zeta_1^* = \frac{2t}{L} - 1$. The analytic form of shifted CPs $\zeta_n^*(t)$ of degree n is defined by

$$\zeta_n^*(t) = n \sum_{i=0}^n (-1)^{n-i} 2^{2i} \frac{\Gamma(n+i)}{\Gamma(2i+1)\Gamma(n-i+1)L^i} t^i. \tag{3.2}$$

With $\zeta_n^*(0) = (-1)^n$, $\zeta_n^*(1) = 1$. Now, the function $S(t)$ is defined in $[0, L]$ and a square integrable function on that interval. So, $S(t)$ can be expressed in terms of shifted CPs of first kind as:

$$S(t) = \sum_{i=0}^{\infty} d_i \zeta_i^*(t). \tag{3.3}$$

Now, for numerical approximation, only the first $(m + 1)$ terms of shifted CPs are considered. Hence, we get

$$S_m(t) = \sum_{i=0}^m d_i \zeta_i^*(t). \tag{3.4}$$

$$D^\alpha S_m(t) = \sum_{i=0}^m d_i D^\alpha (\zeta_i^*(t)). \tag{3.5}$$

So, for $i = 1, 2, \dots, m$,

$$\begin{aligned} D^\alpha (\zeta_i^*(t)) &= i \sum_{k=\lceil \alpha \rceil}^i (-1)^{i-k} 2^{2k} \frac{\Gamma(k+i)}{(2k)!(i-k)!L^i} D^\alpha t^k, \\ &= i \sum_{k=\lceil \alpha \rceil}^i (-1)^{i-k} 2^{2k} \frac{\Gamma(k+i)t^{k-\alpha}}{(i-k)!(k-\alpha)!(2k)!L^i}. \end{aligned} \tag{3.6}$$

Then

$$D^\alpha S_m(t) = \sum_{i=0}^m d_i \Xi_{i,k}, \tag{3.7}$$

where $\Xi_{i,k}$ is presented by

$$\Xi_{i,k} = i \sum_{k=\lceil \alpha \rceil}^i \frac{(-1)^{i-k} 2^{2k} \Gamma(k+i) t^{k-\alpha}}{(i-k)!(k-\alpha)!(2k)!L^i}. \tag{3.8}$$

4. Convergence analysis

Theorem 4.1 ([46]). *Suppose that the function $S(t)$ is so constrained that $S''(t) \in L_2[0, L]$ and $|S''(t)| \leq \epsilon$, where ϵ is a constant. Then the series (3.7) of the shifted Chebyshev expansion is uniformly convergent and:*

$$|d_l| < \frac{\epsilon}{l^2}, \quad (l \in 1, 2, \dots) \tag{4.1}$$

Theorem 4.2 ([46]). *Suppose that $S(t) \in C^m[0, 1]$. Then the error in approximating the function $S(t)$ by $S_m(t)$ by using the formula (3.7) can be bounded by:*

$$\begin{aligned} \|S(t) - S_m(t)\| &\leq \frac{\rho \Delta^{(m+1)}}{(m+1)!}, \\ \text{where } \rho &= \max_{t \in [0,1]} S^{(m+1)}(t), \\ (\Delta &= \max\{t, t - t_0\}). \end{aligned} \tag{4.2}$$

5. SCM for Solving Fractional Order COVID-19 Model

Now, SCM with the help of shifted CPs will be used for solving the systems of fractional order differential equations (1.1) to (1.4) with the given initial conditions. For applying this technique, we have to approximate $S(t)$, $E(t)$, $I(t)$, and $R(t)$. So, we have

$$S_m(t) = \sum_{i=0}^m d_i \zeta_i^*(t), \tag{5.1}$$

$$E_m(t) = \sum_{i=0}^m e_i \zeta_i^*(t), \tag{5.2}$$

$$I_m(t) = \sum_{i=0}^m f_i \zeta_i^*(t), \tag{5.3}$$

$$R_m(t) = \sum_{i=0}^m g_i \zeta_i^*(t). \tag{5.4}$$

Now, there are $m+1 - \lceil \alpha \rceil$ collocation points t_p . Using the collocation points, the above

system of equations can be approximated as:

$$\sum_{i=0}^m \sum_{k=\lceil \alpha \rceil}^i d_i \Xi_{i,k} t_p^{k-\alpha} = a - k \sum_{i=0}^m f_i \zeta_i^*(t_p) - \sum_{i=0}^m d_i \zeta_i^*(t_p) (1 + \alpha \sum_{i=0}^m f_i \zeta_i^*(t_p)) - d_0 \sum_{i=0}^m d_i \zeta_i^*(t_p), \tag{5.5}$$

$$\sum_{i=0}^m \sum_{k=\lceil \alpha \rceil}^i e_i \Xi_{i,k} t_p^{k-\alpha} = k \sum_{i=0}^m f_i \zeta_i^*(t_p) - \sum_{i=0}^m d_i \zeta_i^*(t_p) (1 + \alpha \sum_{i=0}^m f_i \zeta_i^*(t_p)) - (d_0 + \gamma) \sum_{i=0}^m e_i \zeta_i^*(t_p), \tag{5.6}$$

$$\sum_{i=0}^m \sum_{k=\lceil \alpha \rceil}^i f_i \Xi_{i,k} t_p^{k-\alpha} = b + \gamma \sum_{i=0}^m e_i \zeta_i^*(t_p) - (d_0 + \mu + \beta) \sum_{i=0}^m f_i \zeta_i^*(t_p). \tag{5.7}$$

$$\sum_{i=0}^m \sum_{k=\lceil \alpha \rceil}^i g_i \Xi_{i,k} t_p^{k-\alpha} = \beta \sum_{i=0}^m f_i \zeta_i^*(t_p) - d_0 \sum_{i=0}^m g_i \zeta_i^*(t_p). \tag{5.8}$$

In this case, the roots of the shifted CPs $T_m^*(t)$ are taken as collocation points. Now,

we get utilizing the initial conditions

$$\sum_{i=0}^m (-1)^i d_i = \delta_1. \tag{5.9}$$

$$\sum_{i=0}^m (-1)^i e_i = \delta_2. \tag{5.10}$$

$$\sum_{i=0}^m (-1)^i f_i = \delta_3. \tag{5.11}$$

$$\sum_{i=0}^m (-1)^i g_i = \delta_4. \tag{5.12}$$

So, there are total $4m + 4$ no of non-linear system of algebraic equations where the degree of shifted Chebyshev polynomials is denoted by m . Newton's iteration method is used for solving those kind of system of equations to get the values of unknowns d_i , e_i , f_i and g_i , $i = 0, 1, 2, \dots, m$.

6. Numerical Results and Discussion

In this section, we shall discuss the numerical simulation of the given COVID 19 model. Here, spectral collocation method is used for approximating the solution. From Figs. 1-4, we have plotted susceptible components, exposed components, infected components, recovered components for different values of $\alpha = 1, 0.9, 0.8, 0.7$ respectively with the given initial values. Also, the behaviour of different components for different values of $\alpha = 1, 0.8, 0.6, 0.4$ are presented from From Figs. 5-8.

Now, the values in Table1 which is used here are taken from [37]. The data from Table 2 from WHO [47] express the values of different components in different time for India, Pakistan, Bangladesh, Sri-lanka. It shows that susceptibility is reducing which produced the increasing of exposures. So, the infection class is increasing.

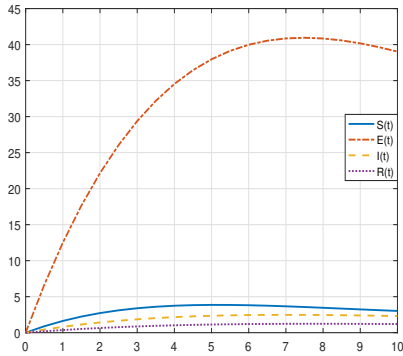


Fig. 1. Plots of $S(t)$, $E(t)$, $I(t)$ and $R(t)$ of the COVID-19 model vs. time for $\alpha = 1$.

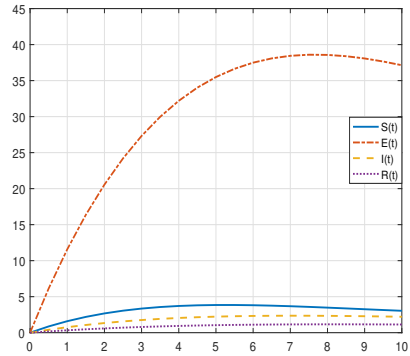


Fig. 4. Plots of $S(t)$, $E(t)$, $I(t)$ and $R(t)$ of the COVID-19 model vs. time for $\alpha = 0.7$.

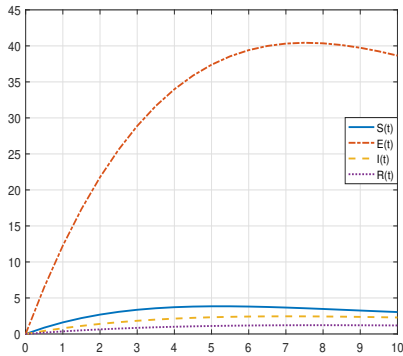


Fig. 2. Plots of $S(t)$, $E(t)$, $I(t)$ and $R(t)$ of the COVID-19 model vs. time for $\alpha = 0.9$.

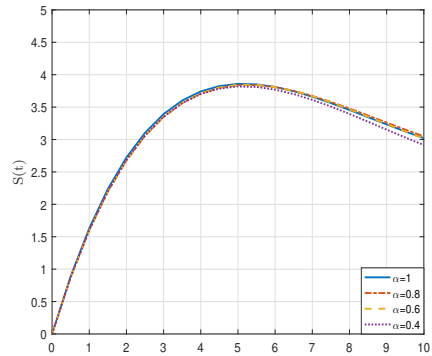


Fig. 5. Plots of $S(t)$ of the COVID-19 model for different values of α .

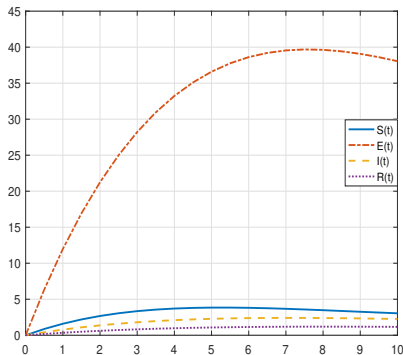


Fig. 3. Plots of $S(t)$, $E(t)$, $I(t)$ and $R(t)$ of the COVID-19 model vs. time for $\alpha = 0.8$.

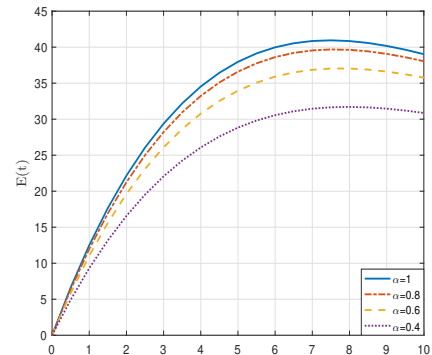


Fig. 6. Plots of $E(t)$ of the COVID-19 model for different values of α .

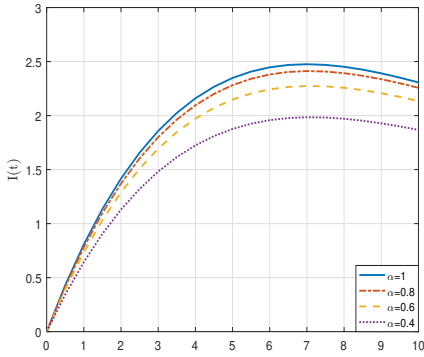


Fig. 7. Plots of $I(t)$ of the COVID-19 model for different values of α .

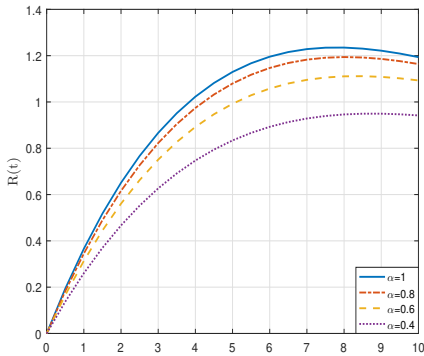


Fig. 8. Plots of $R(t)$ of the COVID-19 model for different values of α .

Also, the cure and the recovery class also are increasing because of more death cases.

In Figs. 9-12, the results for the four different countries are replicated. These show that the precipitability ratio of India is faster than the other countries due to large population as in 9, Pakistan is in second and so on. Here, the susceptible compartment is decreasing with the increasing of exposing. Hence, the rate of infection is increasing because of large population of India. Sri Lanka has less infection flow than Pakistan, Bangladesh as shown in Figs. 10-12 respectively. Also susceptible, exposed, infected and recovered class for different countries are plotted from Figs. 13-16.

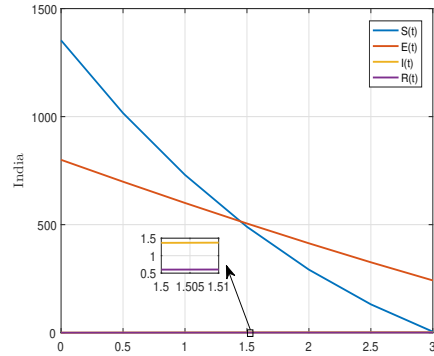


Fig. 9. Plots of $S(t)$, $E(t)$, $I(t)$ and $R(t)$ for the given initial values for India.

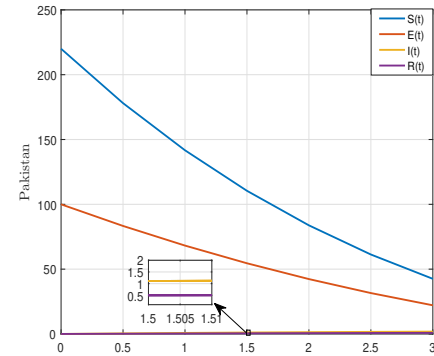


Fig. 10. Plots of $S(t)$, $E(t)$, $I(t)$ and $R(t)$ for the given initial values for Pakistan.

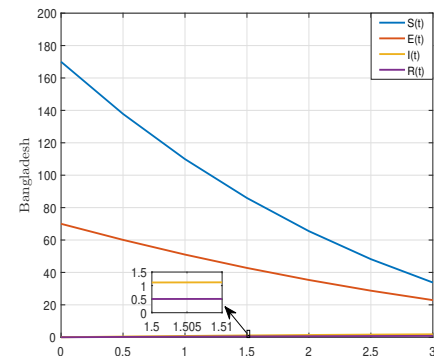


Fig. 11. Plots of $S(t)$, $E(t)$, $I(t)$ and $R(t)$ for the given initial values for Bangladesh.

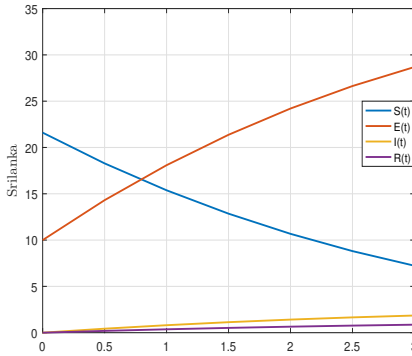


Fig. 12. Plots of $S(t)$, $E(t)$, $I(t)$ and $R(t)$ for the given initial values for Srilanka.

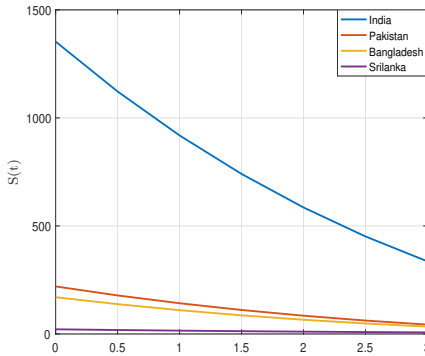


Fig. 13. Plots of $S(t)$ of the COVID-19 model for the given different initial values.

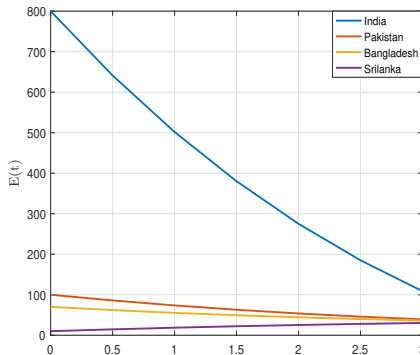


Fig. 14. Plots of $E(t)$ of the COVID-19 model for the given different initial values.

Table 1. Explanation of the parameters with numerical values.

Parameters	Physical interpretation	Values
a_1	Negative cases population	0.73 Millions
d_1	Natural death	0.02
μ_1	Death due to Covid	0.0009
b_1	Population with positive cases	0.06003
α	Individuals lose immunity	0.00009
k_1	Constant of proportionality	0.098601
γ_1	The rate of infection	0.00007
β_1	The rate of recovered	0.01

Table 2. Explanation of the parameters with numerical values.

Parameters	Numerical Values
$S_0(t)$	1353, 220, 170, 21.6 Ms
$E_0(t)$	800, 100, 70, 10 Ms
$I_0(t)$	0.027977, 0.013328, 0.005149, 0.000523 Ms
$R_0(t)$	0.007407, 0.003310, 0.000267, 0.000127 Ms

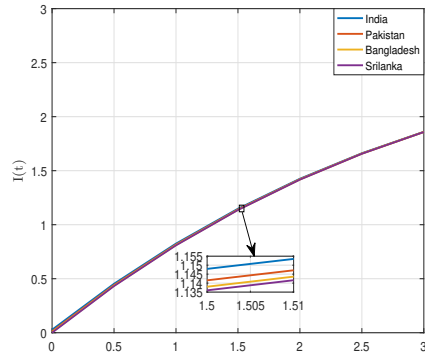


Fig. 15. Plots of $I(t)$ of the COVID-19 model for the given different initial values.

7. Conclusion

COVID-19 model having four components is described here. Also, the solutions are presented using one of the well known numerical technique spectral collocation method. Further, we have simulated

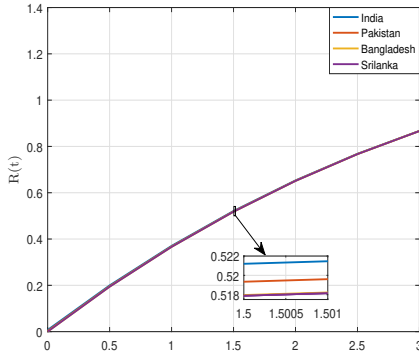


Fig. 16. Plots of $R(t)$ of the COVID-19 model for the given different initial values.

the results for the given different initial conditions with different values of fractional order α . Also, from the graphical representations, it can be said that how the rate of COVID-19 is increasing of India, Srilanka, Pakistan, Bangladesh respectively. At last, we have compared the results with the real data for four different countries. It is presented that the infection spread rates are different for these four countries. We also concluded that spreading rate of India and Pakistan is faster in comparison with other two countries, Bangladesh and Srilanka because of having huge population. In future, We can use this method to solve COVID-19 models having five or six components to get better results.

References

- [1] Jahanshahi H, Yousefpour A, Munoz-Pacheco JM, Moroz I, Wei Z, Castillo O. A new multi-stable fractional-order four dimensional system with self-excited and hidden chaotic attractors: Dynamic analysis and adaptive synchronization using a novel fuzzy adaptive sliding mode control method. *Applied Soft Computing*. 2020;87:105943.
- [2] Soradi S, Jahanshahi H, Yousefpour A, Bekiros S. King algorithm: A novel optimization approach based on variable-order fractional calculus with application in chaotic financial systems. *Chaos, Solitons Fractals*. 2020;132:109569.
- [3] Freeborn TJ. A survey of fractional-order circuit models for biology and biomedicine. *IEEE Journal on emerging and selected topics in circuits and systems*. 2013;3(3):416–424.
- [4] Chen D, Chen YQ, Xue D. Digital fractional order Savitzky-Golay differentiator. *IEEE Transactions on Circuits and Systems II: Express Briefs*. 2011;58(11):758–762.
- [5] Sadeghian H, Salarieh H, Alasty A, Meghdari A. On the fractional-order extended Kalman filter and its application to chaotic cryptography in noisy environment. *Applied Mathematical Modelling*. 2014;38(3):961–973.
- [6] Singh J, BD Kumar D. New aspects of fractional Bloch model associated with composite fractional derivative. *Mathematical Modelling of Natural Phenomena*. 2021;16:1–14.
- [7] Singh J. Analysis of fractional blood alcohol model with composite fractional derivative. *Chaos, Solitons & Fractals*. 2020;140:110127.
- [8] Organization WH. WHO director-general’s opening remarks at the media briefing on covid-19-11 march 2020. 2020. 2020.
- [9] Ferguson N, Laydon D, Nedjati Gilani G, Imai N, Ainslie K, Baguelin M, et al. Report 9: Impact of non-pharmaceutical interventions (NPIs) to reduce COVID-19 mortality and healthcare demand. 2020.
- [10] Wang C, Horby PW, Hayden FG, Gao GF. A novel coronavirus outbreak of global health concern. *The Lancet*. 2020;395(10223):470–473.
- [11] Munster VJ, VDNVRDDWE Koopmans M. A novel coronavirus emerging

- in China—key questions for impact assessment. *New England Journal of Medicine*. 2020;382(8):692–694.
- [12] Huang C, Wang Y, Li X, Ren L, Zhao J, Hu Y, et al. Clinical features of patients infected with 2019 novel coronavirus in Wuhan, China. *The Lancet*. 2020;395(10223):497–506.
- [13] Li Q, Guan X, Wu P, Wang X, Zhou L, Tong Y, et al. Early transmission dynamics in Wuhan, China, of novel coronavirus-infected pneumonia. *New England Journal of Medicine*. 2020.
- [14] Gupta R, Ghosh A, Singh AK, Misra A. Clinical considerations for patients with diabetes in times of COVID-19 epidemic. *Diabetes & metabolic syndrome*. 2020;14(3):211.
- [15] Ma Y, Zhao Y, Liu J, He X, Wang B, Fu S, et al. Effects of temperature variation and humidity on the death of COVID-19 in Wuhan, China. *Science of The Total Environment*. 2020:138226.
- [16] Li X, Wang L, Yan S, Yang F, Xiang L, Zhu J, et al. Clinical characteristics of 25 death cases infected with COVID-19 pneumonia: a retrospective review of medical records in a single medical center, Wuhan, China. *medRxiv*. 2020.
- [17] Lin Q, Zhao S, Gao D, Lou Y, Yang S, Musa SS, et al. A conceptual model for the coronavirus disease 2019 (COVID-19) outbreak in Wuhan, China with individual reaction and governmental action. *International journal of infectious diseases*. 2020.
- [18] Chen TM, Rui J, Wang QP, Zhao ZY, Cui JA, Yin L. A mathematical model for simulating the phase-based transmissibility of a novel coronavirus. *Infectious Diseases of Poverty*. 2020;9(1):1–8.
- [19] Danane J HZNK Allali K. Mathematical analysis and simulation of a stochastic COVID-19 Levy jump model with isolation strategy. *Results in Physics*. 2021;23:103994.
- [20] Hussain G KAIMZGNKAA Khan T. Modeling the dynamics of novel coronavirus (COVID-19) via stochastic epidemic model. *Alexandria Engineering Journal*. 2021;60(4):4121–4130.
- [21] Singh H HZNK Srivastava HM. Numerical simulation and stability analysis for the fractional-order dynamics of COVID-19. *Results in physics*. 2021;20:103722.
- [22] Baba IA NKAAANT Yusuf A. Mathematical model to assess the imposition of lockdown during COVID-19 pandemic. *Results in Physics*. 2021;20:103716.
- [23] Shaikh AS TMNKI Jadhav VS. Analysis of the COVID-19 pandemic spreading in India by an epidemiological model and fractional differential operator. 2020, doi: 1020944/preprints2020050266v1.
- [24] Logeswari K NK Ravichandran C. Mathematical model for spreading of COVID-19 virus with the Mittag-Leffler kernel. *Numerical Methods for Partial Differential Equations*. 2020, doiorg/101002/num22652.
- [25] Shaikh AS NK Shaikh IN. A mathematical model of COVID-19 using fractional derivative: outbreak in India with dynamics of transmission and control. *Advances in Difference Equations*. 2020;2020(1):1–19.
- [26] Naik PA QSZJTS Yavuz M. Modeling and analysis of COVID-19 epidemics with treatment in fractional derivatives using real data from Pakistan. *The European Physical Journal Plus*. 2020;135(10):1–42.
- [27] Yavuz M GFÖF Coşar F. A new mathematical modeling of the COVID-19 pandemic including the vaccination campaign. *Open Journal of Modelling and Simulation*. 2021;9(3):299–321.

- [28] Naik PA YMZJ Owolabi KM. Chaotic dynamics of a fractional order HIV-1 model involving AIDS-related cancer cells. *Chaos, Solitons & Fractals*. 2020;140:110272.
- [29] Yavuz M SN. Stability analysis and numerical computation of the fractional predator–prey model with the harvesting rate. *Fractal and Fractional*. 2020;4(3):35.
- [30] Hammouch Z ÖN Yavuz M. Numerical solutions and synchronization of a variable-order fractional chaotic system. *Mathematical Modelling and Numerical Simulation with Applications (MMNSA)*. 2021;1(1):11–23.
- [31] B D. Stability analysis of an incommensurate fractional-order SIR model. *Mathematical Modelling and Numerical Simulation with Applications (MMNSA)*. 2021;1(1):44–55.
- [32] Naik PA ZJ Yavuz M. The role of prostitution on HIV transmission with memory: A modeling approach. *Alexandria Engineering Journal*. 2020;59(4):2513–2531.
- [33] Yavuz M ÖN. Analysis of an epidemic spreading model with exponential decay law. *Mathematical Sciences and Applications E-Notes*. 2020;8(1):142–154.
- [34] Danane J AKRSSJ Hammouch Z. A fractional-order model of coronavirus disease 2019 (COVID-19) with governmental action and individual reaction. *Mathematical Methods in the Applied Sciences*. 2021, doiorg/101002/mma7759.
- [35] Yadav S SJBD Kumar D. Analysis and dynamics of fractional order Covid-19 model with memory effect. *Results in physics*. 2021;24:104017.
- [36] Bonyah E KDDS Sago AK. Fractional optimal control dynamics of coronavirus model with Mittag–Leffler law. *Ecological Complexity*. 2021;45:100880.
- [37] Ud Din R, Seadawy AR, Shah K, Ullah A, Baleanu D. Study of global dynamics of COVID-19 via a new mathematical model. *Results in Physics*. 2020;19:103468.
- [38] Chen Y, Tang T. Convergence analysis of the Jacobi spectral-collocation methods for Volterra integral equations with a weakly singular kernel. *Mathematics of computation*. 2010;79(269):147–167.
- [39] Yin Z, Gan S. Chebyshev spectral collocation method for stochastic delay differential equations. *Advances in Difference Equations*. 2015;2015(1):113.
- [40] Zayernouri M, Karniadakis GE. Fractional spectral collocation methods for linear and nonlinear variable order FPDEs. *Journal of Computational Physics*. 2015;293:312–338.
- [41] Akbar M. Finite difference and spectral collocation methods for the solution of semilinear time fractional convection-reaction-diffusion equations with time delay. *Journal of Applied Mathematics and Computing*. 2019;61(1-2):635–656.
- [42] Turalska M, West BJ. A search for a spectral technique to solve nonlinear fractional differential equations. *Chaos, Solitons & Fractals*. 2017;102:387–395.
- [43] Kumar S, Ghosh S, Kumar R, Jleli M. A fractional model for population dynamics of two interacting species by using spectral and Hermite wavelets methods. *Numerical Methods for Partial Differential Equations*. 2020, doiorg/101002/num22602.
- [44] Podlubny I. An introduction to fractional derivatives, fractional differential equations, to methods of their solution and some of their applications. *Mathematics in science and engineering*. 1999;198:xxiv+–340.
- [45] Bell WW. *Special functions for scientists and engineers*. Melbourne, Courier Corporation; 2004.

- [46] Khader M, Saad K. A numerical approach for solving the fractional Fisher equation using Chebyshev spectral collocation method. *Chaos Solitons Fractals*. 2018;110:169–177.
- [47] Organization WH. Novel Coronavirus (2019-nCoV) situation reports World Health Organization; 2020.